Syntheses and Crystal Structures of New Ternary Selenides: $Rb_3Yb_7Se_{12}$ and $CsEr_3Se_5$

Sung-Jin Kim* and So-Jung Park

Department of Chemistry, Ewha Womans University, 120-750, Seoul, Korea

Hoseop Yun and Junghwan Do

Department of Chemistry, Ajou University, 441-749, Suwon, Korea

Received February 29, 1996[⊗]

The new compounds $Rb_3Yb_7Se_{12}$ and $CsEr_3Se_5$ have been synthesized through the reaction of elemental rare-earth metal and Se with halide flux at 680 °C. The structures of the compounds were determined by the single-crystal X-ray diffraction method. The structures of $CsEr_3Se_5$ and $Rb_3Yb_7Se_{12}$ are considerably similar to each other. $Rb_3Yb_7Se_{12}$ crystallizes in space group *Pnnm* of the orthorhombic system with cell dimensions $a = 12.385(4)$ Å, $b = 25.688(7)$ Å, $c = 4.063(1)$ Å, and $Z = 2$. $CsEr_3Se_5$ crystallizes in space group *Pnma* of the orthorhombic system with cell dimensions $a = 22.059(9)$ Å, $b = 4.095(2)$ Å, $c = 12.155(5)$ Å, and $Z = 4$. The structures of these compounds have infinite one-dimensional channels. The channels consist of edge-sharing $RESe_6$ (RE = rare-earth metal) octahedral layers and alkali-metal ions reside in the channels. The $RESe_6$ octahedra in both compounds are distorted with bond lengths varing from 2.752(3) Å to 2.939(2) Å. The result of magnetic susceptibility and resistivity measurement of $Rb_3Yb_7Se_{12}$ showed that it is paramegnetic and is an insulator. Structural comparison between $Rb_3Yb_7Se_{12}$ and $CsEr_3Se_5$ is discussed. A series of additional isostructural compounds $Cs_3Y_7Se_{12}$ and $Rb_3Er_7Se_{12}$ have been prepared, and structural diagrams of ternary selenides with respect to cationic radius ratios were drawn.

Introduction

In many of structures of binary and ternary transition or rare-earth metal chalcogenides, the metals are octahedrally coordinated by chalcogens to form MX_6(M = transition or rare-earth metals; X = chalcogens) units and those units are condensed differently by sharing their edges, corners, and their faces. Rock-salt-based transition or rare-earth metal chalcogenides are classical examples of the chalcogenides, and their structures are described in terms of edge-sharing MX_6 octahedral arrays. In the layered MX_2 compounds, each octahedral MX_6 unit shares its six edges in 2-dimensional directions.

The structures adopted by a particular system appear to be crucially influenced by the presence or absence of cations that may reside in the channels or between the layers. In other words, the cations such as alkaline earth metals or alkali metals in ternary chalcogenides may break three dimensionally condensed MX_6 networks into separate clusters or one dimensional chains or two dimensional layers. For example, octahedral NbS_3^{2-} units in $BaNbS_3$ share their trans-faces and form infinite one-dimensional chains which are parallel to the hexagonal *c*-axis. The intrachain metal−metal distances are short enough to form metal−metal bonds; however, the metal chains are separated by large barium cations.[1−3]

Recently, some rare-earth metal chalcogenides have been described as a promising new class of optical materials.[4−6] Following the early works of Flahaut et al.[7,8] on yttrium- and rare-earth-containing ARE_2X_4(A = Ca, Sr, Ba; RE = rare-earth metals, Y; X = chalcogens) compounds, Lowe-ma et al.[6,9] refined the structure of CaY_2S_4, and characterized its optical properties as a potential IR window material. CaY_2S_4 crystallizes in the Yb_3S_4-type structure ($Yb^{2+}Yb^{3+}{}_2S_4$) which is isostructural with $CaYb_2S_4$.[10] The structure is formed of strings of four edge-sharing YS_6 octahedra, and the four edge-sharing strings are interconnected by vertex-sharing to form open channels, where Ca^{2+} ions reside with monocapped trigonal prismatic coordinates. Patrie et al.[8] synthesized a series of ARE_2X_4(X = S, Se; RE = Tb−Lu, Y for Sr; and RE = Nd-Lu, Y for Ba) compounds with $CaFe_2O_4$-type structure.[7,9,10] This structure consists of edge-shared double rutile chains of REX_6 octahedra. The double rutile chains are connected at the vertices to form the channels where Ba^{2+} or Sr^{2+} ions reside with bicapped trigonal prismatic coordinate.

For layered compounds, the AMX_2(A = alkali metals; M = rare-earth or transition metals; X = chalcogens) compounds[11−14] tend to crystallize with a cation-ordered NaCl structure, in which two different cations are ordered in alternating cubic (111) planes. During an attempt to synthesize the AMX_2 compounds

* Author to whom correspondence should be addressed.

[⊗] Abstract published in *Advance ACS Abstracts,* August 1, 1996.

(1) Kim, S.-J.; Bae, H.-S.; Yee, K.-A.; Choy, J.-H.; Kim. D.-K.; Hur, N.-H. *J. Solid State Chem.* **1995**, *115*, 427.
(2) Gardner, R. A.; Vlasse, M.; Wold, A. *Inorg. Chem.* **1969**, *8*, 2784.
(3) Gardner, R. A.; Vlasse, M.; Wold, A. *Acta Crystallogr. Sect. B* **1969**, *25*, 781.
(4) Isaacs, T. J.; Hopkins, R. H.; Kramer, W. E. *J. Electron. Mater.* **1975**, *4*, 1181.
(5) Kumta P. N.; Risbud, S. H. *J. Mater. Sci.* **1994**, *29*, 1135.
(6) Nadler, M. P.; Lowe-Ma, C. K.; Vanderah, T. A. *Mater. Res. Bull.* **1993**, *28*, 1345.
(7) Flahaut, J. *Handbook on the Physics and Chemistry of Rare Earths*; Gschneidner, K. A., Jr., Eyring, L., Eds.; North-Holland: Amsterdam, 1979; Chapter 31, p 1.
(8) Patrie, M.; Golabi, S. M.; Flahaut, J.; Domange, L. *C. R. Acad. Sci. Paris* **1964**, *259*, 4039.
(9) Lowe-Ma, C. K.; Vanderah, T. A. *J. Solid State Chem.* **1995**, *117*, 363.
(10) Carpenter, J. D.; Hwu, S. -J. *J. Solid State Chem.* **1992**, *97*, 332.
(11) Ohtani, T.; Honjo, H.; Wada, H. *Mater. Res. Bull.* **1987**, *22*, 829.
(12) Sato, M.; Adachi, G.; Shiokawa, J. *Mater. Res. Bull.* **1984**, *19*, 1215.
(13) (a) Bronger, W.; Brüggemann, W.; von der Ahe, M.; Schmitz, D. *J. Alloys Compd.* **1993**, *200*, 205. (b) Ballestracci, R.; Bertaut, E. F. *Bull. Soc. Fr. Mineral. Cristallogr.* **1964**, *87*, 512. (c) Ballestracci, R. *Bull. Soc. Fr. Mineral. Cristallogr.* **1965**, *88*, 207. (d) Bronger, W.; Elter, R. ; Maus, E.; Schmitt, T. *Rev. Chim. Miner.* **1973**, *10*, 147.
(14) Plesko, E. P.; White, W. B. *J. Solid State Chem.* **1994**, *112*, 295.

S0020-1669(96)00227-3 CCC: $12.00

using larger cations such as Cs^+ and Rb^+, we found a series of new ternary selenides. The resulted compounds have huge pseudorectangular channels consisting of nine or eight edge-shared octahedral layers. Here, we present the syntheses and full details of this new series of one dimensional ternary selenides, $Rb_3Yb_7Se_{12}$ and $CsEr_3Se_5$, and compare their structures with those of other ternary selenides and sulfides.

Experimental Section

$Rb_3Yb_7Se_{12}$ was prepared from the mixture of Yb chips (Aldrich 99.9%) and Se shot (Aldrich 99.999%) in a molar ratio of 1:2 with an excess amount of RbCl. $CsEr_3Se_5$ was prepared from the mixture of Er chips (Aldrich 99.9%) and Se shot (Aldrich 99.999%) in a molar ratio of 1:2 with an excess amount of CsCl. RbCl or CsCl was used as a flux material and also as a starting binary in these reactions. The reaction mixture was double-sealed in an evacuated quartz tube and heated at 680 °C for 10 days. Then, the heated product was slowly cooled to room temperature. The product was washed with water to remove excess flux. Other isostructural compounds were obtained with similar procedures, for example, CsCl was used for flux to prepare $Cs_3Y_7Se_{12}$, etc.

The reactions lead to the formation of needle-shaped crystals at the surface and within the melt. The excess Se that was not reacted always observed at the cold end of the reaction tube. When a molar ratio of Se/Yb = 1.7 was used for the starting mixture, the best quality of product was obtained. Any observable evidence of side product was not detected by powder X-ray diffraction. The chemical compositions of the crystals were confimed by energy-dispersive X-ray (EDX) using a scanning electron microscope (SEM-Philips XL20, EDX-PV9900), and incorporation of Cl from the flux and Si from the quartz tube was not detected in either phase.

A red $Rb_3Yb_7Se_{12}$ needle with approximate dimensions of 0.016 × 0.03 × 0.40 mm^3 bound by faces of a form {100}{010}{001} was selected for X-ray analysis. Preliminary examination and data collection were performed with Mo Kα_1 radiation (λ = 0.710 73 Å) on an MXC3 diffractometer (Mac Science) equipped with an incident beam monochromator graphite crystal. The unit cell parameter and the orientation matrix for data collection were obtained from the least-squares refinement, using the setting angles of 21 reflections in the range of 17° < 2θ(Mo Kα) < 28°. The orthorhombic cell parameters and calculated volume were a = 12.385(4) Å, b = 25.688(7) Å, c = 4.063(1) Å, and V = 1292.5(6) $Å^3$. The observed Laue symmetry and systematic extinctions ($0kl$,$k + l = 2n + 1$; $h0l$, $h + l = 2n + 1$) were indicative of the space groups D_{2h}^{12}-*Pnnm* or C_{2v}^{10}-*Pnn2*. The centrosymmetric *Pnnm* was assumed, and subsequent refinements confirmed the choice of this space group.

Intensity data were collected with the $\omega-2\theta$ scan technique. The intensities of two standard reflections, measured every 100 reflections, showed no significant deviations during the data collection. The initial positions for all atoms were obtained from the direct methods of the SHELXS-86 program.[15] The structure was refined by full-matrix least-squares techniques with the use of the SHELXL-93 program.[16] Anisotropic thermal motions were included. Once all atoms were located, the occupancies of the Rb sites were allowed to vary throughout the balance of the refinement. The occupancy factors for Rb(1) and Rb(2) were refined to 0.499(6) and 0.264(6), respectively. Consequently, a full occupancy was assigned for the Rb(1) site and a half-occupancy was applied to the Rb(2) site to satisfy the charge neutrality of the compound, $(Rb^+)_3(Yb^{3+})_7(Se^{2-})_{12}$. Because no evidence was found for ordering of the Rb(2) site, a statistically disordered structure is assumed. With the composition established, the data were corrected for absorption with the use of the analytical method of Tompa and de Meulenaer.[17] The final cycle of refinement performed on F_o^2 with 1304 unique reflections afforded residuals wR2($F_o^2 > 0$) = 0.1232, and the conventional R index based on reflections having $F_o^2 > 2\sigma(F_o^2)$ is 0.0440. A difference Fourier synthesis calculated with phase based on the final parameters showed no peak greater than 12% of the height of a Se atom.

Similar procedures were followed for a yellow needle crystal of $CsEr_3Se_5$. The orthorhombic cell parameters and calculated volume were a = 22.059(9) Å, b = 4.095(2) Å, c = 12.155(5) Å, and V = 1097.9(4) $Å^3$. The observed Laue symmetry and systematic extinctions were indicative of the space groups D_{2h}^{16}-*Pnma* or C_{2v}^{9}-*Pn2$_1$a*. The centrosymmetric *Pnma* was assumed, and subsequent refinements confirmed the choice of this space group. Letting occupation factors varying on the Cs site did not lead to any significant change in the occupation factor. Thus, this compound can be formulated as $Cs^+(Er^{3+})_3(Se^{2-})_5$. Crystallographic data for $Rb_3Yb_7Se_{12}$ and $CsEr_3Se_5$ are given in Table 1. Tables 2 and 3 list positional parameters and equivalent isotropic thermal parameters for $Rb_3Yb_7Se_{12}$ and $CsEr_3Se_5$ respectively. Selected bond distances and angles for $Rb_3Yb_7Se_{12}$ and $CsEr_3Se_5$ are listed in Tables 4−7, respectively. Complete tables of bond lengths and angles for the two compounds are available as Supporting Information.

Table 1. Crystallographic Data for $Rb_3Yb_7Se_{12}$ and $CsEr_3Se_5$

	$Rb_3Yb_7Se_{12}$	$CsEr_3Se_5$
fw	2415.20	1029.49
cryst syst	orthorhombic	orthorhombic
space group	D_{2h}^{12}-*Pnnm*	$^{D}{}_{2h}{}^{16}$-*Pnma*
a (Å)	12.385(4)	22.059(9)
b (Å)	25.688(7)	4.095(2)
c (Å)	4.063(1)	12.155(5)
V ($Å^3$)	1292.5(6)	1097.9(4)
Z	2	4
D_{calc} (g/cm^3)	6.206	3.751
temp (K)	293(2)	298(2)
wavelength (Å)	0.71073	0.71073
μ (mm^{-1})	47.553	42.49
R1 ($F_o^2 > 2\sigma(F_o2)$)[a]	0.0440	0.0482
wR2 ($F_o^2 > 0$)[b]	0.1232	0.1347

[a] R1 = $[\sum||F_o| - |F_c||]/[\sum|F_o|]$. [b] wR2 = $\{[\sum w(F_o^2 - F_c^2)^2]/[\sum w(F_o^2)^2]\}^{1/2}$.

Table 2. Atomic Coordinates and Equivalent Isotropic Displacement Parameters ($Å^2$) for $Rb_3Yb_7Se_{12}$

atom	x	y	z	occupancy (%)	U(eq)[a]
Rb1	0.7875(2)	0.1324(1)	0.5	100	0.022(1)
Rb2	0.5632(5)	0.0295(2)	0	50	0.026(1)
Yb1	0.2192(1)	0.0834(1)	0	100	0.011(1)
Yb2	0.0908(1)	0.2119(1)	0.5	100	0.011(1)
Yb3	0.4236(1)	0.1822(1)	0.5	100	0.011(1)
Yb4	0	0	0.5	100	0.010(1)
Se1	0.2551(2)	0.1961(1)	0	100	0.010(1)
Se2	0.0677(2)	0.1034(1)	0.5	100	0.010(1)
Se3	0.3744(2)	0.0769(1)	0.5	100	0.012(1)
Se4	0.3460(2)	0.4799(1)	0.5	100	0.012(1)
Se5	0.4405(2)	0.2890(1)	0.5	100	0.010(1)
Se6	0.0777(2)	0.3214(1)	0.5	100	0.012(1)

[a] U(eq) is defined as one-third of the trace of the orthogonalized $\mathbf{U}_{ij}$ tensor.

Table 3. Atomic Coordinates and Equivalent Isotropic Displacement Parameters ($Å^2$) for $CsEr_3Se_5$

atom	x	y	z	occupancy (%)	U(eq)[a]
Cs1	0.09006(8)	0.25	0.8569(1)	100	0.0251(5)
Er1	0.19717(5)	0.25	0.54491(9)	100	0.0108(4)
Er2	0.32471(5)	0.75	0.70147(9)	100	0.0106(4)
Er3	0.05381(5)	0.75	0.39017(9)	100	0.0104(4)
Se1	0.1976(1)	0.75	0.6984(2)	100	0.0119(6)
Se2	0.1841(1)	0.75	0.3742(2)	100	0.0101(6)
Se3	0.3241(1)	0.25	0.5466(2)	100	0.0114(6)
Se4	0.4521(1)	0.75	0.7307(2)	100	0.0119(6)
Se5	0.0688(1)	0.25	0.5532(2)	100	0.0103(5)

[a] U(eq) is defined as one-third of the trace of the orthogonalized $\mathbf{U}_{ij}$ tensor.

(15) Sheldrick, G. M. *Acta Crystallogr.* **1990**, *A46*, 467.
(16) Sheldrick, G. M. *SHELXL 93, Program for the Refinement of Crystal Structures*; University of Gottingen, Gottingen, Germany, 1993.
(17) de Meulenaer, J.; Tompa, H. *Acta Crystallogr.* **1965**, *19*, 1014.

Table 4. Selected Bond Distances(Å) for $Rb_3Yb_7Se_{12}$

Rb1−Se distances		Rb2−Se distances	
Rb1−Se5(2)	3.433(3)	Rb2−Se3(2)	3.328(5)
Rb1−Se6(2)	3.505(3)	Rb2−Se3(2)	3.493(5)
Rb1−Se2	3.549(4)	Rb2−Se4	3.511(6)
Rb1−Se4(2)	3.602(3)	Rb2−Se6	3.834(6)
Yb1−Se distances		**Yb2−Se distances**	
Yb1−Se4	2.779(3)	Yb2−Se5(2)	2.755(2)
Yb1−Se3(2)	2.801(2)	Yb2−Se2	2.802(3)
Yb1−Se2(2)	2.813(2)	Yb2−Se6	2.817(3)
Yb1−Se1	2.929(3)	Yb2−Se1(2)	2.904(2)
Yb3−Se distances		**Yb4−Se distances**	
Yb3−Se5	2.752(3)	Yb4−Se2(2)	2.785(2)
Yb3−Se3	2.772(3)	Yb4−Se4(4)	2.834(2)
Yb3−Se6(2)	2.789(2)		
Yb3−Se1(2)	2.934(2)		

Table 5. Selected Bond Angles (deg) for $Rb_3Yb_7Se_{12}$

Yb1		Yb2	
Se4−Yb1−Se3(2)	98.22(6)	Se5−Yb2−Se5	95.00(8)
Se3−Yb1−Se3	92.96(9)	Se5−Yb2−Se2(2)	85.56(6)
Se4−Yb1−Se2(2)	88.90(6)	Se5−Yb2−Se6(2)	88.26(6)
Se3−Yb1−Se2(2)	172.83(8)	Se2−Yb2−Se6	170.85(9)
Se3−Yb1−Se2(2)	86.84(6)	Se5−Yb2−Se1(2)	171.09(7)
Se2−Yb1−Se2	92.45(8)	Se5−Yb2−Se1(2)	87.50(5)
Se4−Yb1−Se1	171.81(8)	Se2−Yb2−Se1(2)	86.12(6)
Se3−Yb1−Se1(2)	87.39(6)	Se6−Yb2−Se1(2)	100.37(6)
Se2−Yb1−Se1(2)	85.44(6)	Se1−Yb2−Se1	88.77(8)
Yb3		**Yb4**	
Se5−Yb3−Se3	171.68(9)	Se2−Yb4−Se2	180.0
Se5−Yb3−Se6(2)	88.92(6)	Se2−Yb4−Se4(4)	88.36(6)
Se3−Yb3−Se6(2)	96.76(6)	Se2−Yb4−Se4(4)	91.64(6)
Se6−Yb3−Se6	93.50(9)	Se4−Yb4−Se4(2)	180.0
Se5−Yb3−Se1(2)	86.17(6)	Se4−Yb4−Se4(2)	91.60(8)
Se3−Yb3−Se1(2)	87.83(6)	Se4−Yb4−Se4(2)	88.40(8)
Se6−Yb3−Se1(2)	174.33(7)		
Se6−Yb3−Se1(2)	89.22(5)		
Se1−Yb3−Se1	87.64(8)		

Table 6. Selected Bond Distances (Å) for $CsEr_3Se_5$

Cs−Se distances		Er1−Se distances	
Cs−Se3(2)	3.618(3)	Er1−Se1(2)	2.770(2)
Cs−Se1(2)	3.678(3)	Er1−Se3	2.800(3)
Cs−Se5	3.722(3)	Er1−Se5	2.834(3)
Cs−Se4(2)	3.819(3)	Er1−Se2(2)	2.929(2)
Er2−Se distances		**Er3−Se distances**	
Er2−Se3(2)	2.782(2)	Er3−Se5	2.791(3)
Er2−Se1	2.805(3)	Er3−Se4(2)	2.823(2)
Er2−Se4	2.833(3)	Er3−Se5(2)	2.868(2)
Er2−Se2(2)	2.939(2)	Er3−Se2	2.880(3)

X-ray powder diffraction patterns for those compounds were analyzed using Rietveld-type method[18] (Supporting Information).

Electrical resistivities were measured using the four-probe method and single crystals. For low temperature (liquid nitrogen range) resistivity measurement, four gold wires were connected to the crystal by silver paste. A dc magnetic susceptibility measurement was carried out for $Rb_3Yb_7Se_{12}$ and $Cs_3Y_7Se_{12}$ at temperatures ranging from 5 to 300 K using a Quantum Design SQUID magnetometer.

Results and Discussion

Figure 1 shows a polyhedral representation of $Rb_3Yb_7Se_{12}$, which is projected along the short *c* axis. The structure of this compound can be described as composed of nine edge-sharing octahedra ribbons, and these ribbons are jointed by edge-sharing on both ends and two waists to form open channels. In point of extent of sharing edges, the structure of $Rb_3Yb_7Se_{12}$ is intermediate between the 3-dimensional rock salt structure and layered transition metal dichalcogenides. In the rock salt type transition metal chalcogenides MX (M = transition metals; X = chalcogens), octahedral MX_6 clusters are condensed by sharing all of their 12 edges. However, in transition metal dichalcogenides with the $CdCl_2$-type structure, MX_6 clusters are condensed to form infinite sheets by sharing their six edges in planar directions. Thus, there are no direct polyhedral linkages between the adjacent sheets, and each layer is connected to the next by the weak van der Waals bonds. In $Rb_3Yb_7Se_{12}$, there are four kinds of MX_6 octahedra, and the numbers of edges sharing with neighbors were between that in the rock salt structure and that in the $CdCl_2$ structure.

The structure of a compound is influenced by the size of cations imbedded in interstitials or replaced in transition metal sites. The 3-dimensional edge-shared MX_6 units can be separated by cations into isolated clusters or infinitely connected chains or layers. For example, when alkali metal ions are substituted into half of the M metal sites in rock salt type MX compounds, the alkali metal cations can separate MX_2 layers to form α-$NaFeO_2$-type AMX_2 compounds (Figure 2).[7,11] In these compounds, the cations are small enough to replace the M metal site, even though the charge of the alkali metal ion is different from that of the parent M metals. The A site cation is six-coordinated with respect to chalcogen atoms.

In $Rb_3Yb_7Se_{12}$, the 3-dimensional edge-shared networks in the rock salt structure are partially broken by the Rb^+ cation to form open channels with a quasi-rectangular shape. The Rb^+ cations residing in channels exhibit coordination number 7 (Rb(1)) with a monocapped trigonal prismatic shape and 6 (Rb(2)) with trigonal prismatic shape (Figure 3). The Rb-Se distances range from 3.328(5) to 3.834(6) Å with an average of 3.509 Å. Rb(1) is coordinated by five Se atoms at relatively short distances ranging from 3.433 to 3.549 Å and by two Se atoms at a longer distance of 3.602 Å. Rb(2) in the trigonal prismatic site is coordinated by five Se atoms at distances ranging from 3.328 to 3.511 Å and by one Se atom at the relatively longer distance of 3.834 Å. The mirror contains Rb(1) and Se(2) and the geometry of the $RbSe_7$ polyhedron is similar to that of the CaS_7 polyhedron in CaY_2S_4. In the Rb(2)Se_6 unit, Se(4), Rb(2), and Se(6) lie in a mirror plane.

The $Rb_3Yb_7Se_{12}$ structure contains four crystallographically unique Yb atoms as shown in Figure 4. The four-Yb-centered octahedra unit Yb_4Se_{17} is related to neighboring Yb_4Se_{17} units by a diagonal glide plane perpendicular to *a* axis. If we take a maximum distance of 2.934 Å, all four Yb atoms are six coordinate and all Yb−Se distances range from 2.752(3) to 2.934(2) Å with average of 2.823 Å. This value is in good agreement with the sum of the ionic radii[19] for Se^{2-} and Yb^{3+}-(2.85 Å). As compared to the ideal values of 90 and 180° for cis and trans Se−Yb−Se angles, the cis Se−Yb−Se angles in octahedra range from 85.44° to 100.37° and trans Se−Yb−Se angles range from 170.85 to 180°. The shape of open channel is not exactly rectangular, thus distortion of $YbSe_6$ octahedral seems to be the necessary consequence of the way the channels are formed. The numbers of edge shared with neighboring octahedra are 8, 7, 7, and 6 for Yb(1); Yb(2); Yb(3); and Yb(4)-centered octahedra, respectively. Thus, this structure could be described as an intermediate structure with a 3-dimensional network structure and a layered structure. For example, in reference to the local structure, the Yb(1) is more similar to the

(18) Rietveld, H. M. *J. Appl. Crystallogr.* **1969**, *2*, 65.

(19) Shannon, R. D. *Acta Crystallogr.* **1976**, *A32*, 751.

Table 7. Selected Bond Angles (deg) for $CsEr_3Se_5$

Er1		Er2		Er3	
Se1−Er1−Se1	95.31(8)	Se3−Er2−Se3	94.79(9)	Se4−Er3−Se5(2)	97.16(6)
Se3−Er1−Se1(2)	89.53(6)	Se1−Er2−Se3(2)	89.22(6)	Se4−Er3−Se4	92.98(9)
Se5−Er1−Se1(2)	88.83(6)	Se4−Er2−Se3(2)	95.13(6)	Se5−Er3−Se5(2)	86.63(6)
Se5−Er1−Se3	177.57(8)	Se4−Er2−Se1	173.57(8)	Se5−Er3−Se4(2)	175.99(8)
Se2−Er1−Se1(2)	173.74(7)	Se2−Er2−Se3(2)	174.90(6)	Se5−Er3−Se4(2)	87.83(6)
Se2−Er1−Se1(2)	87.76(6)	Se2−Er2−Se3(2)	88.31(6)	Se5−Er3−Se5	91.10(8)
Se2−Er1−Se3(2)	95.96(6)	Se2−Er2−Se1(2)	86.77(6)	Se2−Er3−Se5	169.57(8)
Se2−Er1−Se5(2)	85.77(6)	Se2−Er2−Se4(2)	88.61(6)	Se2−Er3−Se4(2)	89.99(6)
Se2−Er1−Se2	88.68(8)	Se2−Er2−Se2	88.32(7)	Se2−Er3−Se5(2)	86.08(6)

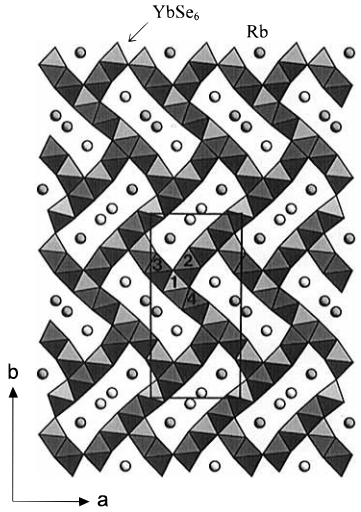

Figure 1. Crystal structure of $Rb_3Yb_7Se_{12}$ projected along the *c* axis in the polyhedral representation. The connectivity of the $YbSe_6$ octahedra is illustrated. Circles represent the Rb atoms. The atom-numberings of asymmetric Yb atoms in octahedral centers are given. The shadings with different contrast on atom and octahedron indicate different heights along the *c* axis.

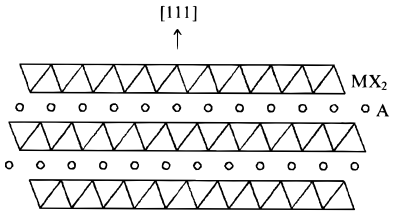

Figure 2. Crystal structure of an α-$NaFeO_2$-type AMX_2 compound showing cubic (111) alternating planes. Circles represent A cations. M-centered octahedrons of MX_6 are connected to form MX_2 layers.

metals of rock salt type compounds and the Yb(4) is more similar to those of $CdCl_2$-type chalcogenides.

There are two crystallographically different Rb^+ sites. During the refinement of the structural model, it became obvious that one of the Rb^+ sites was not fully occupied. The radius of Rb^+ seems too large to fill all of the Rb(2) sites. The final composition deduced from the final refinement was $Rb_3Yb_7Se_{12}$. The structural details of $Cs_3Y_7Se_{12}$ and $Rb_3Er_7Se_{12}$ were very similar to those of $Rb_3Yb_7Se_{12}$ in a number of features described above. The orthorhombic cell parameters for those $Rb_3Yb_7Se_{12}$-type compounds are listed in Table 8.

The structures of $CsEr_3Se_5$ and $Rb_3Yb_7Se_{12}$ are considerably similar to each other as shown in Figure 5. The structure building unit of both compounds is $RESe_6$ and the sizes of the channel in octahedra units are 5 × 4 and 6 × 4, respectively. The Er equivalent to Yb(4) in $Rb_3Yb_7Se_{12}$ is missing in $CsEr_3Se_5$ and that reduces the size of the channel in $CsEr_3Se_5$. More octahedrons are fused to make the channel in $Rb_3Yb_7Se_{12}$ to accommodate three smaller Rb cations per channel. In other words, the size of the Cs^+ cation is large enough so that only

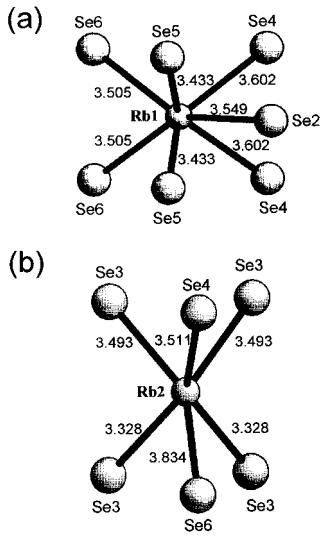

Figure 3. (a) Rb(1)Se_7 polyhedron and (b) Rb(2)Se_6 polyhedron in the $Rb_3Yb_7Se_{12}$ structure. Rb-Se bond lengths are given in Å.

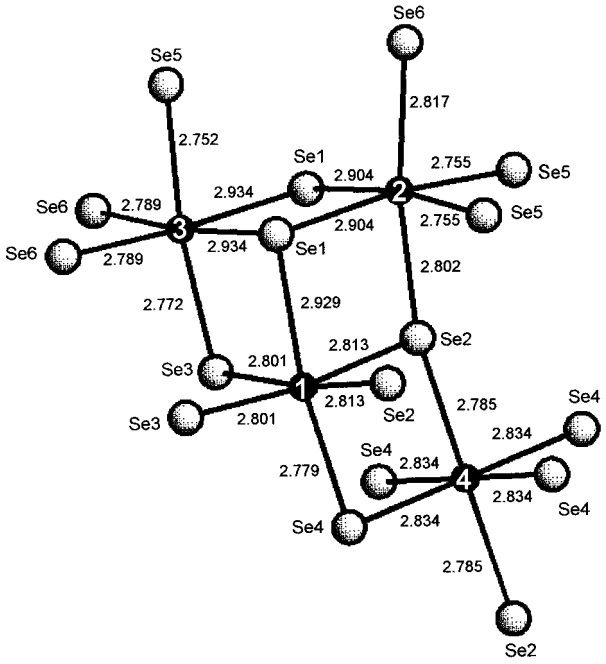

Figure 4. Asymmetric four octahedra condensed unit, Yb_4Se_{17}, of $Rb_3Yb_7Se_{12}$.

two symmetrically equivalent cations can fill the pseudorectangular channels of $CsEr_3Se_5$.

The Cs^+ cations accommodated in channels exhibit a coordination number of 7 with a monocapped trigonal prismatic shape (Figure 6). The geometry of Cs^+ is similar to that of Rb(1) in $Rb_3Yb_7Se_{12}$. The Cs−Se distances range from 3.618(3) to 3.819(3) Å with average of 3.707 Å. Cs^+ is coordinated by five Se atoms at relatively short distances ranging from

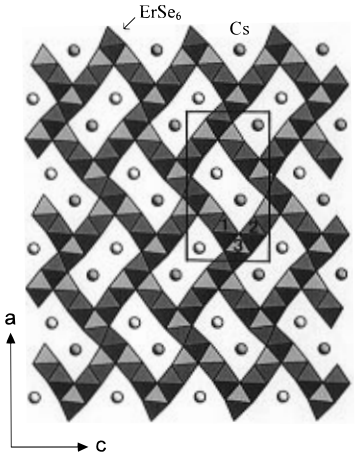

Figure 5. Crystal structure of $CsEr_3Se_5$ projected along the *b* axis in the polyhedral representation. The connectivity of the $ErSe_6$ octahedra is illustrated. Circles represent the Cs atoms. The atom-numberings of asymmetric Er atoms in octahedral centers are given. The shadings with different contrast on atom and octahedron indicate different heights along the *b* axis.

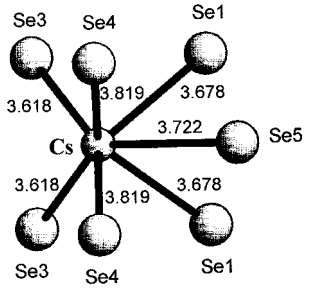

Figure 6. $CsSe_7$ polyhedron in the $CsEr_3Se_5$ structure. Cs−Se bond lengths are given in angstroms.

Table 8. Orthorhombic Cell Parameters (Å) for $A_3Re_7Se_{12}$

	a	*b*	*c*
$Rb_3Yb_7Se_{12}$	12.385(4)	25.688(7)	4.063(1)
$Rb_3Er_7Se_{12}$	12.52(2)	26.02(4)	4.094(7)
$Cs_3Y_7Se_{12}$	12.744(5)	26.288(9)	4.139(2)

3.618(3) to 3.722(3) Å and by two Se atoms at a longer distance of 3.819(3) Å.

The $CsEr_3Se_5$ structure contains three crystallographically unique Er atoms, which is compared to four unique Yb atoms in $Rb_3Yb_7Se_{12}$ (Figure 7). If we take a maximum distance of 2.939 Å, all three Er atoms are six coordinate and all Er−Se distances range from 2.770(3) Å to 2.939(2) Å with an average of 2.843 Å. This value is in good agreement with the sum of the ionic radii for Se^{2-} and Er^{3+} (2.87 Å). As compared to the ideal values of 90 and 180°, the cis Se−Er−Se angles in octahedra range from 85.77(6) to 97.16(6)° and trans Se−Er−Se angles range from 169.57(8) to 177.57(8)°. The numbers of edges shared with neighboring octahedra are 7, 7, and 8 for Er(1)-, Er(2)-, and Er(3)-centered octahedra, respectively.

In the procedure of refinement of the structural model, it became obvious that the Cs^+ site was fully occupied. The size of the channel seems proper to accommodate two Cs^+ ions. The final composition deduced from the final refinement was $CsEr_3Se_5$. The relative mole ratio of RE/Se (RE = rare earth metals) is almost the same in $CsEr_3Se_5$ and $Rb_3Yb_7Se_{12}$; thus, their structure seems to be solely dependent on the relative sizes of cations. The yields of both compounds were very high (∼90%) for each reaction, and the X-ray powder patterns taken from the product after washing out the excess flux show one phase (X-ray pattern in Supporting Information).

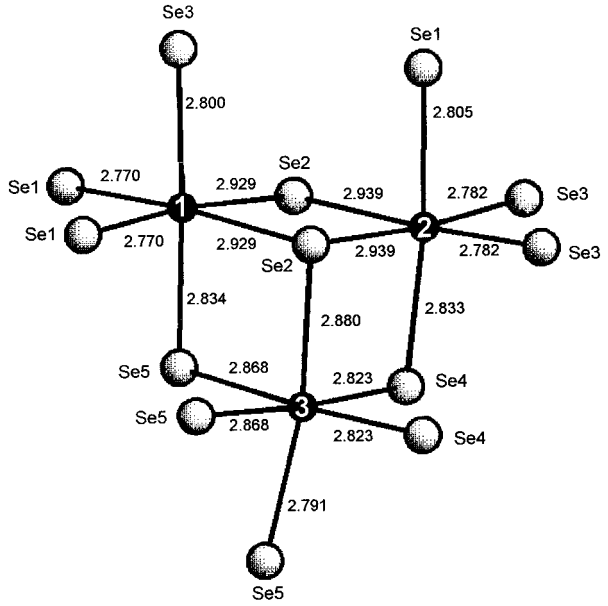

Figure 7. Asymmetric three-octahedra condensed unit, Er_3Se_{13}, of $CsEr_3Se_5$.

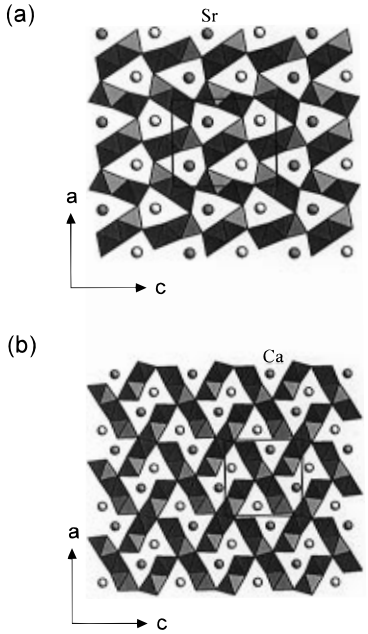

Figure 8. Comparison of (a) SrY_2S_4 and (b) CaY_2S_4 structures.

It has been reported that CaY_2S_4 has the low-temperature Yb_3S_4-type ($Yb^{2+}Yb^{3+}{}_2S_4$) structure in which Yb^{2+} is substituted by Ca^{2+} in the position of 7-coordination.[10] However, SrY_2S_4 and BaY_2S_4 with larger A-type cations were found to have the $CaFe_2O_4$-type structure, and these two sulfides are chalcogenide analogs of this oxide.[10] The sizes and shapes of channels which accommodate cations are different in Yb_3S_4 and $CaFe_2O_4$-type chalcogenides (Figure 8). The shape of channel made by sulfurs in BaY_2S_4 and SrY_2S_4 is pseudotriangular, in which Sr^{2+} or Ba^{2+} is properly fitted in 8-coordinate site of S atoms, with six shorter bonds and two slighly longer bonds (Figure 8a). However, the size of such pseudotriangular channels seems to be too large to accommodate the smaller Ca^{2+} ion; thus fused double triangular shape channels are formed in CaY_2S_4 to accommodate two Ca^{2+} cations (Figure 8b). The coordination number of the smaller cation Ca^{2+} is 7 in the fused double channels.

Both structures of Yb_3S_4-type and $CaFe_2O_4$-type compounds feature three-dimensional frameworks built of edge- and corner-

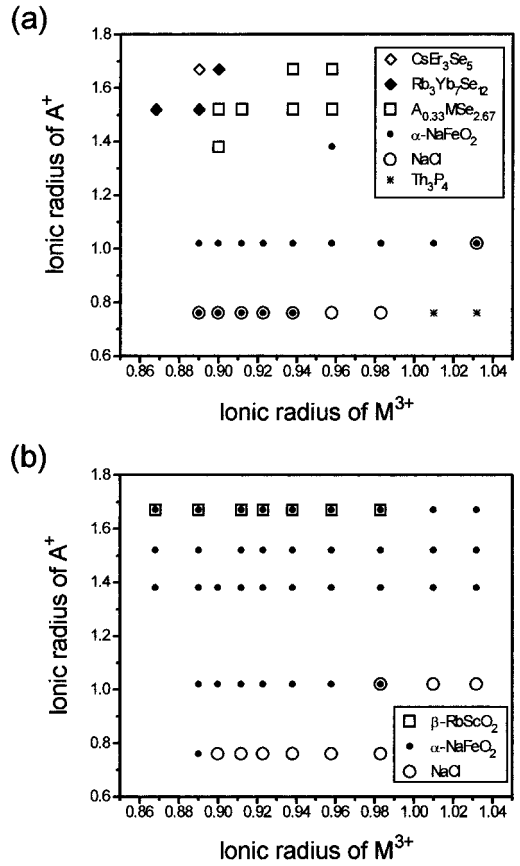

Figure 9. (a) Structural diagram of ternary selenide systems.[7,11,13,20,21] The structure of Th_3P_4 is a defect NaCl-type structure. (b) Structural diagram of ternary sulfide systems.[7,13] The structure of β-$RbScO_2$ is a modified structure of α-$NaFeO_2$. Radii (Å) are Shannon crystal radii for 6-coordination. The resulting separation of structure types suggests that the sizes of cations are important in determining structure type.

sharing YS_6 octahedra. However, the frameworks of newly synthesized $Rb_3Yb_7Se_{12}$-type are built of only edge-sharing $YbSe_6$ octahedra and the size of the channel is much larger than that of the known ternary sulfides. The success of obtaining a new ternary compound is evidently related to the size of the anion as well as the cationic size.

During the attempt to synthesize new compounds using various rare-earth element and halide fluxes, we obtained different layered ternary selenides such as $A_{0.33}MSe_{2.67}$ (A = alkali metals; M = rare-earth or transition metals)[20,21] and $AMSe_2$. The mole ratio of M/Se in $AMSe_2$ is similar to that of above two selenides. Even though the composition of $A_{0.33}MSe_{2.67}$ is different from the title compounds, this compound can be obtained from the same starting composition of Se/M = 2 for certain choices of A^+ and M^{3+} cations. Thus, we included this compound in the following discussion. In $A_{0.33}MSe_{2.67}$, a two-atoms-thick NaCl-type layer and two Se sheets with A cations sandwiched are intergrown. We could draw the structural diagram according to the radius ratios of cations (Figure 9a). In this diagram, a relatively clear separation between $AMSe_2$ and the new structures is observed, and this indicates that the cationic size determines the structure adopted.

When we consider the radius ratio of two cations $r_{A^+}/r_{M^{3+}}$, $AMSe_2$ compounds were synthesized with the NaCl-type or the α-$NaFeO_2$ structure for the smallest $r_{A^+}/r_{M^{3+}}$ value. For smaller values in this region, the compounds crystallize with a disordered NaCl-type structure in which two different cations are statistically distributed in the cation sites. With increasing radius ratio, the compounds tend to crystallize with α-$NaFeO_2$, in which two different cations are segregated on the alternate (111) cubic plane to form a layered structure.[7,11] When larger cations such as Cs^+ and Rb^+ are used (the $r_{A^+}/r_{M^{3+}}$ ratio has a slightly larger value than that of $AMSe_2$), 1-dimensional compounds, $Rb_3Yb_7Se_{12}$ and $CsEr_3Se_5$, were formed at the same reaction temperature. These two new compounds with different structures have almost the same RE/Se composition.

Table 9. Comparison of Coordination Numbers in Ternary Rare-Earth Metal Chalcogenides

Compound (Structure-type)	$LiErS_2$ (α-$NaFeO_2$)	$Cs_3Y_7Se_{12}$ ($Rb_3Yb_7Se_{12}$)	$CsEr_3Se_5$ ($CsEr_3Se_5$)	CaY_2S_4 (Yb_3S_4)	SrY_2S_4 ($CaFe_2O_4$)
Central atom		Ligand atom			
	S	Se	Se	S	S
Re	6	6	6	6	6
A	6	6, 7	7	7	8
Central atom		Ligand atom			
	Li Er	Cs Y	Cs Er	Ca Y	Sr Y
X1	3 3	0 5	2 3	3 2	2 3
X2		1 4	0 5	2 3	
X3		2 3	2 3	2 3	
X4		3 3	2 3	0 4	
X5		2 3	1 4		
X6		3 3			

The structural diagram of sulfides based on earlier works is shown in Figure 9b to compare it with that of ternary selenides. In case of alkali metal ternary sulfides, only two structural types are observed for a wide range of $r_{A^+}/r_{M^{3+}}$ ratios, and the separation between the two structures is clear.

Generally, a reduction in size of the A cations causes the reduction of coordination numbers; thus it finally affects the structures adopted by the compounds (Table 9). The main difference found between alkali metal ternary sulfides and selenides is the coordination number of the anions. In alkali metal ternary sulfides, the sulfurs coordinate to six cations, i.e., three alkali metal and three rare-earth metal cations. However, in selenides, the coordination numbers of selenium vary from 5 to 6, which seems to be related to the greater covalency of selenium (Table 9).

Magnetic susceptibility measurement of $Rb_3Yb_7Se_{12}$ shows that it is paramagnetic with $\mu_{eff} = 4.69\ \mu_B$. The effective magnetic moment of Yb^{3+} with $4f^{13}$ is known to be 4.54 μ_B; thus, the oxidation state of ytterbium in this compound is Yb^{3+}. $Cs_3Y_7Se_{12}$ was a diamagnetic material. The electronic resistivity measurements showed that these new title compounds are insulators.

Conclusions

The new ternary compounds $Rb_3Yb_7Se_{12}$ and $CsEr_3Se_5$ were synthesized, and single crystal structures were solved. The relative mole ratio of RE/Se (RE = rare earth metal) is almost the same in $CsEr_3Se_5$ and $Rb_3Yb_7Se_{12}$, and their adopted structures seem to be solely dependent on the sizes of the metal cations. Also, the success of obtaining a new ternary compound is evidently related to the size of the anion as well as the cationic size. The frameworks of both compounds are built of only edge-sharing $RESe_6$ octahedra and the sizes of channel cross sections in octahedral units were 5 × 4 and 6 × 4, respectively.

The difference found between alkali metal ternary sulfides and selenides is the coordination number of the anions. In ternary sulfides, only two structural types are observed for a wide range of $r_{A^+}/r_{M^{3+}}$ ratios, and in both structures the sulfurs are coordinated by six cations, i.e., three alkali metal and three

(20) Foran, B.; Lee, S.; Aronson, M. C. *Chem. Mater.* **1993**, *5*, 974.
(21) (a) Kim, S. -J.; Oh, H. -J. *Bull. Korean Chem. Soc.* **1995**, *16*, 515. (b) Kim, S.-J.; Park, S.-J. to be published.

rare-earth metal cations. However, in selenides, the coordination numbers of selenium vary from 5 to 6, which seems to be related to the higher covalency of selenium. The structural and magnetic information indicates that the bondings between Se and a rare-earth metal cation have ionic character and the oxidation state of the rare-earth metal is 3+.

Acknowledgment. This work was supported in part by the Korean Ministry of Education (BSRI 95-3413) and Center for Inorganic Materials Chemistry, 1995.

Supporting Information Available: Tables of detailed crystallographic data, anisotropic displacement parameters, and bond lengths and angles for $Rb_3Yb_7Se_{12}$ and $CsEr_3Se_5$, tables of detailed crystallographic data, atomic coordinates, temperature factors, and bond lengths and angles for $Cs_3Y_7Se_{12}$, and a figure showing the results of powder X-ray diffraction refinement with the Rietveld-method for $Rb_3Yb_7Se_{12}$ (16 pages). Ordering information is given on any current masthead page.

IC960227O